Published in final edited form as:
Nanomedicine. 2012 November ; 8(8): 1301–1308. doi:10.1016/j.nano.2012.02.002.

Novel Thermogelling Dispersions of Polymer Nanoparticles for Controlled Protein Release

Tong Cai, (PhD)[†], **Peter D. Hu**[‡,+], **Manwu Sun, (MS)**[‡], **Jun Zhou, (PhD)**[‡], **Yi-Ting Tsai, (MS)**[‡], **David Baker, (BA)**[‡], and **Liping Tang, (PhD)**[‡,*]

[†]Departments of Physics, University of North Texas, Denton TX 76203

[‡]Bioengineering Department, University of Texas at Arlington, Arlington, TX 76019

[+]Texas Academy of Mathematics and Science, Denton, Texas 76201

Abstract

A novel poly(oligo(ethylene glycol) methyl ether methacrylate-co-oligo(ethylene glycol) ethyl ether methacrylate)/ poly(acrylic acid) interpenetrating network (IPN) nanoparticle was synthesized. The temperature-responsive properties of the IPN nanoparticles were investigated by dynamic light scattering method. Atomic force microscopic images confirm the homogenous and mono-disperse morphology of the IPN nanoparticles. Both visual observation and viscosity testing demonstrated that the IPN nanoparticles exhibit thermogelling properties at body temperature, 37°C. Subsequent studies verified that such temperature sensitive properties of IPN nanoparticles allow their ease of injection and then slow release of model proteins, both *in vitro* and *in vivo*. Histological analysis showed that our IPN implants exerted minimal inflammation following subcutaneous implantation. Our results support that, by simply mixing with proteins of interest, the novel IPN nanoparticles can be used to form *in situ* thermogelling devices for controlled protein release.

Keywords

Temperature-sensitive nanoparticle; injectable; thermogelling; controlled drug release

Background

Therapeutic proteins are critically important for treating various diseases. In order to maintain their therapeutic concentrations, carriers have been developed which can be loaded with and then release these beneficial proteins slowly. There have however been several long standing challenges facing such systems. One such deterrent is the fact that fabrication of slow release carriers typically requires the use of solvent(s) which tend to denature and inactivate proteins.[1] This may be overcome during the protein carriers/implants fabrication, by taking advantage of an inverse thermoreversible gelation effect in an aqueous environment at body temperature (37°C).[2] At room temperature, the dispersion should be a

[*]Correspondence to Liping Tang, Ph.D., Bioengineering Department, University of Texas at Arlington, P.O. Box 19138, Arlington, TX 76019-0138. Fax: 817-272-2251; ltang@uta.edu.

No conflict of interests is present

fluid so that proteins can be easily mixed with it. As the protein-loaded dispersion is injected into the human body, the dispersion would gel to delay the diffusion and to cause slow release of the trapped proteins/drugs. These goals have led to the production of many injectable hydrogel scaffolds made of materials including poly(ethylene oxide)-poly(propylene oxide)-poly(ethylene oxide) triblock copolymers (Pluronic or Poloxamer)[3–5] and copolymers of poly-N-isopropylacrylamide-co-acrylic acid (PNIPAM-co-AAc).[6]

Recently, thermosensitive nano- or micro-size particles have emerged as building blocks for thermogelling scaffolds. In addition, the interpenetrating network (IPN) nanoparticles composed of PNIPAM network and poly(acrylic acid) (PAAc) networks were synthesized and found to exhibit a unique thermoreversible gelation property.[7,8] One of the major advantages of PNIPAM-IPN-PAAc nanoparticles over the PNIPAM-co-PAAc copolymer is that the phase transition temperature is independent of the amount of PAAc, whereas random copolymerization results in increasing LCST of the system and depends upon increasing amounts of PAAc.[9] Most recently, poly(*N*-isopropylacrylamide-*co*-2-hydroxyethyl methacrylate) (PNIPAM-co-HEMA) nanoparticle dispersions was synthesized to form macroscopic hydrogels in the presence of $CaCl_2$ upon heating to body temperature. Compared to linear or branched polymers, nano/micro-size particles have some potential advantages including reduced viscosity and better mechanical properties at the same concentration.[10] Although these thermogelling systems exhibit excellent thermally-induced gelling properties, major concerns have been raised in recent years on the long term safety of PNIPAM or PNIPAM-based polymers. Specifically, it has been shown that small amide derivatives generated by the degradation and/or hydrolysis of PNIPAM or PNIPAM-based polymers are carcinogenic and have neural and reproductive toxicity in various animal models[11,12] Therefore, the main driving force of this work is to develop new hydrogel materials with physical, chemical and biological properties that resemble PNIPAM-based hydrogels while avoiding the long-term toxicity complications.

To search for alternative polymers to make IPN nanoparticles, we chose to fabricate IPN hydrogel using polyethylene glycol (PEG)-based polymer. It is well established that PEG is nontoxic and also non-immunogenic.[13,14] Among available PEG-based polymers, we have used oligomers composed of a (meth)acrylate moiety connected to a short poly(ethylene glycol) (POEGMA) chain. These polymers have been shown to possess thermoresponsive properties[15,16] and are useful for fabricating microgels with a variety of particle radii.[17] Here we report the synthesis of a novel thermogelling PEG-based IPN nanoparticle composed of poly(oligo(ethylene glycol)) network and poly(acrylic acid) network. The effect of temperature and pH on their thermogelling properties was studied. Furthermore, using *in vitro* and *in vivo* models, we assessed the controlled protein release properties of the PEG-based IPN nanoparticles. Finally, the tissue compatibility of the PEG-based IPN nanoparticles in the subcutaneous cavity of the mice was evaluated.

Methods

Materials

Methacryloyl-L-Lysine was purchased from Polysciences (Nile, IL). Texas red dye-conjugated dextran (Mw=70 K) was purchased from Invitrogen (Carlsbad, CA). Poly(ethylene glycol) methyl ether methacrylate (MW=300 g/mol, MEO_4MA), poly(ethylene glycol) ethyl ether methacrylate (MW=246g/mol, OEGEEM), ethylene glycol dimethacrylate (EGDMA), ammonium persulfate (APS), acrylic acid (AAc), N, N'-methylenebisacrylamide (BIS), sodium dodecyl sulphate (SDS), N, N, N', N', tetramethyl-ethylenediamine (TEMED), insulin and bovine serum albumin were all purchased from Sigma Aldrich (St Louis, MO). High-molecular weight poly (L-lactic acid) (PLLA, 137 kDa), was obtained from Birmingham Polymers (Birmingham, AL, USA). Near infrared dye

Oyster®-800 was bought from Boca Scientific (Boca Raton, FL). BCA protein assay reagents were purchased from Thermo Fisher Scientific Inc. (Rockford, IL).

Preparation of poly(oligo(ethylene glycol)) nanoparticles

Poly(oligo(ethylene glycol)) nanoparticles were prepared using a precipitation polymerization method.[17] Specifically, OEGEEM (6.5×10^{-2}M), MEO_4MA (7.25×10^{-3}M), along with EGDMA (2.5×10^{-4}M) as a crosslinking agent, SDS (7.0×10^{-4}M), and methacryloyl-l-lysine (6.45×10^{-3}M) were all dissolved in distilled water in a three-neck flask, the flask was placed in a circulating bath of water at 70°C under nitrogen gas for 30 minutes. Polymerization was initiated by adding APS (1.75×10^{-1}M) and the reactions were carried out at 70°C for 6 hours under N_2 gas. The resultant poly(oligo(ethylene glycol)) nanoparticles were purified with dialysis against DI water for one week.

Preparation of PEG-based IPN nanoparticles

The above-prepared nanoparticles were then used as seeds to form a second network based on polyacrylic acid (PAAc). Acrylic acid (1.68×10^{-1}M) and BIS (7.6×10^{-3}M) were both dissolved in poly(oligo(ethylene glycol)) nanoparticle solution (20 mg/ml) in a flask at 23°C for 24 hours. By adding TEMED (3.44×10^{-1}M) and APS (1.75×10^{-1}M), the reaction was carried out in a nitrogen environment for 30 min. The resultant nanoparticles were purified by dialyzing against DI water for one week and then divided into two groups for either physical characterization or drug release/biocompatibility studies.

The concentration (wt%) of IPN nanoparticles was determined using standard evaporation method.[7] Briefly, a weighted IPN nanoparticle dispersion(W_{IPN}) was dried for one week at 60°C in a circulation oven and further dried for one week at 60°C in a vacuum oven, the final weight of dried IPN nanoparticles(W'_{IPN}) was obtained. Therefore, the concentrations of IPN nanoparticles were calculated by the method. The composition of IPN nanoparticle was estimated using a thermogravimetric analyzer (TGA Q50, TA instruments, New Castle, DE).[18] Samples of dried poly(oligo(ethylene glycol)) nanoparticles, poly(acrylic acid) and IPN nanoparticles were heated in a platinum pan from room temperature to 600°C at a heating rate of 10°C/min under nitrogen atmosphere. The weight ratio of the PAAc component to the poly(oligo(ethylene glycol)) component was determined by decomposition curve of each samples as previously described.

Atomic force microscopy

PEG-based IPN nanoparticles were imaged using Veeco Digital Instruments Nanoscope III AFM (Plainview, NY) set on tapping mode as described earlier.[8] All test samples were prepared by casting several drops of the dispersion onto a slide and allowed to dry.

Dynamic light scattering characterization

The sizes of PEG-based IPN nanoparticles were characterized with a dynamic light scattering spectrometer (ALV, Germany) at a scattering angle of 90°. The instrument is equipped with an ALV-5000 digital time correlator and a helium-neon laser (Uniphase 1145P, output power of 22 mW and wavelength of 632.8 nm) as the light source. For dynamic light scattering (DLS) measurements, the intensity-intensity correlation function $G^{(2)}(\tau, \theta)$ was measured, which was related to the normalized first-order electric field time correlation function $|g^{(1)}(\tau, \theta)|$ as depicted by the Siegert relation[19,20]

$$G^{(2)}(\tau,\theta)=<I(0,\theta)\, I(\tau,\theta)>=A[1+\beta\left|g^{(1)}(\tau,\theta)\right|^2] \quad (1)$$

where τ is the delay time, A is measured base line, and β is the coherent factor the detection. For a polydisperse sample, $|g^{(1)}(\tau, \theta)|$ is related to the decay rate (Γ) distribution $G(\Gamma)$

$$\left|g^{(1)}(\tau,\theta)\right| = \quad (2)$$

In this study, c$G(\Gamma)$ was calculated using both the CONTIN program developed by Provencher[21]. The relaxation rate Γ was a function of both the colloidal concentration C and the scattering vector q. For a diffusive relaxation at infinite dilution of colloids, these effects were expressed as

$$\Gamma/q^2 = D \quad (3)$$

where D was the translational diffusion coefficient at $C \rightarrow 0$ and $q \rightarrow 0$, which was related to the hydrodynamic radius (R_h) by the Stokes-Einstein equation, $R_h = kT/6\pi\eta D$, where k, η, and T are the Boltzmann constant, the solvent viscosity, and the absolute temperature, respectively. The DLS measurements were carried out at the scattering angle θ =90°. More detailed description about both static and dynamic light scattering measurements can be found in our previous publication.[22]

Viscosity measurements

The viscosity of the PEG-based IPN nanoparticles was measured as a function of temperature with ATS Viscoanalyser (ATS RheoSystems, Bordentown, NJ). The sample holder had two parallel plates, each with a plate diameter of 25 cm, and a gap of 0.5mm between the two plates. The constant stress was set at 10 Pa. During the experiments, a solvent trap was applied to prevent water evaporation. The data were collected and analyzed with RheoExplorer v5.0 software as described earlier.[8]

In vivo biocompatibility tests

In this study, all animal experiments and care were performed in accordance with the University of Texas at Arlington Animal Care and Use Committee (IACUC). We tested the extent of tissue responses to particles with different properties using a mouse implantation model. Three types of materials were included in the study. These are poly(oligo(ethylene glycol)) nanoparticles, their IPN nanoparticles, and poly-L-lactic Acid (PLLA) microparticles as control. PLLA microparticles were synthesized according to a modified precipitation method with an average size of 15 μm.[23] For the biocompatibility test, 8–12 week old BALB/C mice (male, 20–25 gram body weight, Taconic Farms, Inc., Germantown, NY) were implanted subcutaneously via 19 gauge syringe needle with 0.5 ml of particles. After implantation for 2 weeks, implant-bearing mice were sacrificed and the implants as well as surrounding tissues were then frozen, sectioned and placed on poly-L-lysine coated slides. To assess the extent of tissue responses to various particles, some of these slides were H&E stained. Stained sections were imaged using a Leica fluorescence microscope (Leica Microsystems, Wetzlar, GmbH) equipped with a CCD Camera (Retiga EXi, QImage). All staining samples were analyzed using NIH ImageJ to assess the extent of implant-mediated cellular responses using established procedures.[24–26]

In vitro controlled drug and protein release

For *in vitro* assessment of its drug release properties, centrifuged PEG-based IPN nanoparticles (10 wt%) were adjusted to 5 wt% IPN nanoparticle dispersion with 25mg Texas red dye-conjugated dextran (4mg/ml) at 21°C with phosphate buffered saline (PBS, pH 7.4). After increasing the temperature to 37°C, the IPN dispersion became a solid gel and 1 ml of 10 mM phosphate buffered saline (PBS, pH 7.4) was then added on top of the solid

gel. The slow release properties of the dextran-embedded IPN nanoparticles were documented with images at different time points.

In a separate study, insulin was selected as a model protein for quantifying the slow release property of PEG-based IPN nanoparticle dispersion. For that, insulin (0.5 μg) was mixed with 50 μg of IPN nanoparticles at room temperature. After incubating at 37°C for 30 minutes to form a solid gel, 1 ml of PBS was added to each sample. At each time point, 500 μl of the solution was collected for protein measurements using BCA protein colorimetric assay based on the manufacturer's instructions. The amount of insulin in solution at different time points was determined based on a linear standard curve established with insulin controls. The standard relationship between UV absorption peak value and insulin concentration is represented by a linear equation: $y = 0.0011x + 0.0467$ with $R_2 = 0.983$.

In vivo controlled protein release measurement using imaging system

For *in vivo* protein release, we used Oyster800-labeled bovine serum albumin (BSA) as a model protein. BSA-Oyster800 was produced by conjugation of near infrared dye, Oyster®-800, with BSA following the manufacturer's instruction.[27] Briefly, 100 mg of BSA and 1mg of Oyster®-800 were dissolved in 4ml and 2ml of 10 mM PBS buffer (pH 7.4), respectively. The two solutions were mixed together for 6 hours at room temperature in the dark. The Oyster800-conjugated BSA was dialyzed prior to the experiments. Controlled release experiments were performed on 8–12 week old BALB/C mice (male, 20–25 gram body weight, Taconic Farms, Inc., Germantown, NY). 400 μg of BSA-Oyster800 was respectively mixed with 100 ul of PEG-based IPN nanoparticle dispersion at a polymer concentration of 0%, 3% and 5% (wt %), and then injected subcutaneously in the back of a mouse. At specific time points, the mice were anesthetized with isoflurane inhalation and then imaged at excitation wavelength of 760nm and emission wavelength of 830nm by the KODAK *In vivo* FX Pro (Kodak, USA). The same polygon ROIs were drawn over the implantation locations in the fluorescence imaging. The mean intensities for all pixels in the fluorescence imaging were calculated to evaluate the release rate.

Statistical Analyses

Data was expressed as mean ± SD and groups were compared using Student t-test. Differences were considered statistically significant when $p < 0.05$.

Results

Synthesis and characterization of PEG-based IPN hydrogel nanoparticles

Poly(oligo(ethylene glycol)) nanoparticles were synthesized using a precipitation polymerization method. Using poly(oligo(ethylene glycol)) nanoparticles as the templates, the IPN nanoparticles were also prepared by template polymerization of acrylic acid in poly(oligo(ethylene glycol)) nanoparticle solution. The weight ratio of the PAAc component to the poly(oligo(ethylene glycol)) component is estimated to be ~ 0.43 by the gravimetric method. Figure 1A shows the average radius and size distribution of poly(oligo(ethylene glycol)) and its IPN nanoparticles, measured using dynamic light scattering at 21°C. It is estimated that size the distributions of both poly(oligo(ethylene glycol)) and its IPN nanoparticles are narrow and their average radii are 78 nm and 150 nm, respectively (Figure 1A). The larger radius of the IPN particle indicates that the PAAc network was added onto poly(oligo(ethylene glycol)) nanoparticles. AFM images further confirm that, under dehydration, both poly(oligo(ethylene glycol)) and IPN nanoparticles are rather homogenous and spherical in shape (Figure 1B). The decrease in particle sizes is due to their shrinkage during the drying process for the preparation of AFM samples. The temperature-dependent particle size change for poly(oligo(ethylene glycol)) and its IPN nanoparticles was also

determined by dynamic light scattering (Figure 1C). Our results show that the poly(oligo(ethylene glycol)) shrinks the most with a LCST of 29°C and that the radius of IPN particles shrinks less above the LCST. It should be noted that the size of the IPN nanoparticles at low temperature and body temperature are very similar. Such minimal size changes may be caused by the phenomenon described earlier[28] that the physical presence of temperature-insensitive poly(acrylic acid) network hinders the deswelling of IPN nanoparticles compared to its parental - poly(oligo(ethylene glycol)) nanoparticles.

Interestingly, an aqueous dispersion of IPN nanoparticles with 5% wt concentration undergoes a transformation from a low-viscous fluid to a solid-like gel when heated above the gelation temperature at which the dispersion exhibits a drastic increase in viscosity. As shown in Figure 2A, at 37°C, the dispersion in the test tube is physically gelled and cannot flow out even by inversion of the tube. The temperature-dependent viscosity of the aqueous dispersion of the IPN nanoparticles was then measured and compared with that of the control poly(oligo(ethylene glycol)) dispersion (Figure 2B). The viscosity of the poly(oligo(ethylene glycol)) nanoparticle dispersion decreased as the temperature increased and leveled off above 29°C. This was due to the reduction of particle size with increasing temperature.

The thermogelling effect is not only temperature-dependent but also pH-dependent. At 37°C, the dispersion of IPN nanoparticles remained in liquid form at pH = 4 but became a solid-like gel at pH = 7.0 (Figure 2B). The pH-dependent gelling effect is caused by an ionization of PAAc. At pH 7, ionized PAAc provides adequate support for the poly(oligo(ethylene glycol)) network.

Biocompatibility of PEG-based IPN hydrogel nanoparticles

Biocompatibility of IPN hydrogel nanoparticles was assessed using a mouse subcutaneous implantation model.[24,25,29] After implantation for 2 weeks, the implants and surrounding tissues were recovered for histological analyses, quantification and comparison. We compared tissue responses to three types of particles – PLLA microparticles, poly(oligo(ethylene glycol)) and its IPN nanoparticles. Interestingly, we found that both poly(oligo(ethylene glycol)) nanoparticles and its IPN nanoparticles prompted similar and mild tissue responses (Figure 3A). The low tissue response to poly(oligo(ethylene glycol)) nanoparticles is consistent with many earlier works which show the tissue and blood compatibility of PEG or PEG-coated nanoparticles.[30–32] On the other hand, PLLA particles prompt substantially stronger tissue responses accompanied by increased cellular infiltration inside the particle implants (Figure 3A). By quantifying the capsule thickness, we found that capsule thickness triggered by PLLA implants (~40μm) is 40% less than by poly(oligo(ethylene glycol)) nanoparticles (~66μm) and its IPN nanoparticle implants (~59μm) (Figure 3B). Furthermore, by quantifying cell infiltration depth, we found that PLLA implants prompt 50% more cell infiltration depth (~360μm) than poly(oligo(ethylene glycol)) nanoparticles (~210μm) and its IPN nanoparticle implants (~195μm) (Figure 3C). Interestingly, we find that most of the recruited cells accumulated in the capsule region of both types of PEG-based implants (Figure 3A). It appears that IPN nanoparticle implants possess good tissue compatibility.

Controlled release properties of PEG-based IPN hydrogel nanoparticles *in vitro*

This IPN nanoparticle dispersion was then tested for its ability to slowly release the protein. Visual observations on the controlled release properties of IPN nanoparticle dispersion was first performed by mixing Texas red dye-conjugated dextran (MW: 70 K) with the IPN nanoparticles at 21°C (Figure 4A). After raising the temperature to 37°C, the dye-loaded dispersion became a solid-like gel. PBS solution was then placed on top of the gel to

monitor the release of dye-conjugated dextran. A faint purple color can be seen in the PBS solution after 3 hours, demonstrating that some dye was released from the solid gel (Figure 4B). After incubation for 120 hours at 37°C, substantially more dye was found in the PBS while the solid-like gel became a lighter purple hue (Figure 4C). Finally, after removal of the PBS, the solid gel was cooled to 21°C at which it changed to a fluid (Figure 4D). A light purple color in the dispersion indicated that the dye was not completely released even after 120 hours (Figure 4D). This increasing presence of dye in the solution indicates that the IPN nanoparticles are able to release the dye-conjugated dextran slowly for a long period of time, perhaps ≥ 120 hours.

Subsequent studies were carried out to assess the ability of the IPN nanoparticle dispersion to release insulin. Following the identical procedure stated above, insulin was mixed and trapped in IPN nanoparticle dispersion at 37°C before adding PBS on top of the solid-like gel. By measuring the insulin amounts in PBS, we were able to calculate the cumulative percentage (%) of insulin release from the solid-like gel. Indeed, our results support that the IPN nanoparticle dispersion has good protein slow release properties. About 30% of insulin released within the first 2 hours. However, the majority of the insulin (~75%) was released in an almost linear and constant rate between 1 – 150 hours (Figure 4E).

In vivo protein release properties of PEG-based IPN hydrogel nanoparticles

Animal testing has long been the gold standard for assessing the properties of controlled release devices.[33,34] However, many animals are often needed to obtain reliable comparisons between different devices. In recent years, real-time molecular imaging has developed as an effective tool for monitoring cellular and protein responses *in vivo*.[35,36] Limited studies were also done to continuously monitor the release of drugs in live animals.[37,38] Taking advantage of these developments, we performed studies to determine the slow release properties of IPN nanoparticles and also investigate the effect of polymer content on the protein release rate. For that, Oyster800-conjugated BSA was used as model protein and mixed with different percentages (0, 3, and 5%) of IPN nanoparticles at room temperature and then injected subcutaneously on the back of the same animal. Immediately after implantation, strong fluorescence signals were observed at all three injection sites. Through comparison of images taken in series at different time points, we found that BSA in saline quickly disappeared from the injection site at day 1, while 3% IPN nanoparticles showed prolonged release of BSA for about 3 days (Figure 5A). In the meanwhile, 5% IPN nanoparticles demonstrated a substantially slower release rate and had 10% residual BSA at day 5 (Figure 5A). By quantifying the amount of residual BSA based on fluorescence intensities, our results clearly demonstrate the slow protein release properties of IPN nanoparticles (Figure 5B). Specifically, we observed a ~39% release of BSA from 5 wt% IPN nanoparticles while 54% and 65% of BSA release was found to be associated with 3 wt % IPN nanoparticles and saline control 6 hrs after implantation, respectively. The quick release of BSA from the saline control is anticipated.

Discussion

In this study, a novel thermogelling IPN nanoparticle composed of a poly(oligo(ethylene glycol)) and poly(acrylic acid) network has been developed using template polymerization technique.[7,39,40] These novel PEG-based IPN nanoparticles possessed good thermogelation properties, although the mechanism(s) governing PEG-based IPN nanoparticle formation has yet to be determined. There are at least two potential processes governing such particle formation. First, the hydrogen bonded complex formation between the ether oxygen of poly(oligo(ethylene glycol)) nanoparticle and -COOH of acrylic acid contributes the growth of PAAc network within poly(oligo(ethylene glycol)) network as described earlier.[41,42] Second, hydrogen bonding and ionic interactions may also be created between the amine

groups of the poly(oligo(ethylene glycol)) nanoparticles and the carboxyl groups of PAAc as previously documented.[28,39,40,43] Furthermore, we are still in the process of uncovering the thermogelation mechanism of the IPN nanoparticles. Based on our observations and several recent publications,[45–46] we assume that the thermogelation of PEG-based IPN nanoparticles is mediated by temperature-dependent hydrophobic interactions. Specifically, as that temperature stays below the LCST of the thermoresponsive segments, these nanoparticles remain to be hydrophilic and thus stay in liquid form. When the temperature rises above the LCST, poly(OEGEEM-*co*-MEO_4MA) segments of the IPN nanoparticles become hydrophobic which lead to precipitation and gelation as shown in recent findings.[44,45]

Using a subcutaneous implantation model, our results have confirmed that the PEG-based IPN nanoparticle gel prompted substantially less inflammatory responses than PLLA microparticles. In addition, minimal cell infiltration was found in IPN nanoparticle gel implants. Since PEG has cell repellant properties,[46] poly(oligo(ethylene glycol)) nanoparticles and their derived products are likely to inhibit the infiltration of cells into the IPN implants. In addition, it is well established that PEG-derivatives are non-toxic and non-immunogenic.[13,14] We thus assumed that the degradation products of the PEG-based IPN nanoparticle gel would not exert cell toxicity similar to those of PNIPAM-based hydrogels.

Further studies also revealed that, at 37°C, IPN nanoparticles exhibited slow release of dye-conjugated dextran (≥ 120 hours) and insulin (~150 hours). It should be noted that the release rates of dye-conjugated dextran from IPN nanoparticles are substantially lower than dextran release rates from other hydrogel systems, including PNIPAM-IPN-PAAc system[28] and β-Cyclodextrin hydrogel.[47] In addition, a steady, continuous release of insulin is a preferable property for stable protein delivery as revealed in previous studies.[48–50] Interestingly, we have also observed that the slow release rates varied greatly shortly after gelation (~ first 60 minutes). The detailed mechanism causing such variation is not clear. Several lines of evidence suggest that, during the gelation process, drugs/proteins may be separated from the gel and then isolated in the small compartments between solidified polymers. The distribution and location of these compartments may vary significantly between different samples/preparations which may lead to large variation of the protein release at the first 60 minutes.

To determine the slow release properties of IPN nanoparticles *in vivo*, NIR dye-conjugated BSA was used in the investigation. We found that the release of BSA from IPN nanoparticles was polymer concentration dependent. IPN gel with higher polymer percentage (5%) released in slower rate and longer duration than lower percentage's (3%) IPN gel. In the determination of the influence of particle concentration on protein release rate, the time in which 50% of the loaded drug being released from IPN nanoparticle networks was defined as the characterized times (τ). τ for control was 4 h, whereas τ for 3% and 5% gel significantly increased and was found to be 6 h and 12 h, respectively. These results support our hypothesis that the thermogelling network becomes a solid-like gel at body temperature. Such transformation trapped and slowed down the diffusion rate of BSA. Furthermore, the higher polymer percentage reduced pore size between nanoparticles and reduced the release rate of entrapped proteins. This finding is in agreement with an earlier study in which the higher particle concentration resulted in a slower release.[28]

Overall, our studies have shown that poly(oligo(ethylene glycol))-based IPN nanoparticles were successfully synthesized. Such nanoparticles can be made to exhibit excellent pH-dependent thermogelling effects. Our results support that IPN nanoparticles triggered minimal tissue responses and inhibited cell infiltration similar to PEG nanoparticles. The IPN dispersions can be easily mixed and then used as a biocompatible carrier for controlled

release of proteins both *in vitro* and *in vivo*. Furthermore, the rate of drug release is able to be tuned by changing concentration of IPN nanoparticles. Overall, our results suggest the great potential of the PEG-based IPN nanoparticles in protein therapy and drug delivery.

Acknowledgments

This work was supported by a NIH grant RO1 EB007271. PDH acknowledges the Summer Research Scholarship by Texas Academy of Mathematics and Science.

References

1. Peppas NA, Langer R. New challenges in biomaterials. Science. 1994; 263:1715–1720. [PubMed: 8134835]
2. Ron ES, Bromberg LE. Temperature-responsive gels and thermogelling polymer matrices for protein and peptide delivery. Adv Drug Deliv Rev. 1998; 31:197–221. [PubMed: 10837626]
3. Alexandridis P, Hatton TA. Poly(Ethylene Oxide)-Poly(Propylene Oxide)-Poly(Ethylene Oxide) Block-Copolymer Surfactants in Aqueous-Solutions and at Interfaces - Thermodynamics, Structure, Dynamics, and Modeling. Colloid Surface A. 1995; 96:1–46.
4. Kim YJ, Choi S, Koh JJ, Lee M, Ko KS, Kim SW. Controlled release of insulin from injectable biodegradable triblock copolymer. Pharm Res. 2001; 18:548–550. [PubMed: 11451045]
5. Jeong B, Kim SW, Bae YH. Thermosensitive sol-gel reversible hydrogels. Adv Drug Deliv Rev. 2002; 54:37–51. [PubMed: 11755705]
6. Stile RA, Healy KE. Poly(N-isopropylacrylamide)-based semi-interpenetrating polymer networks for tissue engineering applications. 1. Effects of linear poly(acrylic acid) chains on phase behavior. Biomacromolecules. 2002; 3:591–600. [PubMed: 12005532]
7. Xia XH, Hu ZB. Synthesis and light scattering study of microgels with interpenetrating polymer networks. Langmuir. 2004; 20:2094–2098. [PubMed: 15835657]
8. Zhou J, Wang G, Zou L, Tang L, Marquez M, Hu ZB. Viscoelastic behavior and in vivo release study of microgel dispersions with inverse thermoreversible gelation. Biomacromolecules. 2008; 9:142–148. [PubMed: 18067257]
9. Hirotsu S, Hirokawa Y, Tanaka T. Volume-Phase Transitions of Ionized NIsopropylacrylamide Gels. J Chem Phys. 1987; 87:1392–1395.
10. Gan TT, Zhang YJ, Guan Y. In Situ Gelation of P(NIPAM-HEMA) Microgel Dispersion and Its Applications as Injectable 3D Cell Scaffold. Biomacromolecules. 2009; 10:1410–1415. [PubMed: 19366198]
11. Ankareddi I, Bailey MM, Brazel CS, Rasco JE, Hood RD. Developmental toxicity assessment of thermoresponsive poly(N-isopropylacrylamide-Co-acrylamide) oligomers in CD-1 mice. Birth Defects Res B Dev Reprod Toxicol. 2008; 83:112–116. [PubMed: 18395840]
12. Dimitrov I, Trzebicka B, Muller AHE, Dworak A, Tsvetanov CB. Thermosensitive water-soluble copolymers with doubly responsive reversibly interacting entities. Prog Polym Sci. 2007; 32:1275–1343.
13. Duncan R. The dawning era of polymer therapeutics. Nat Rev Drug Discov. 2003; 2:347–360. [PubMed: 12750738]
14. Greenwald RB, Choe YH, McGuire J, Conover CD. Effective drug delivery by PEGylated drug conjugates. Adv Drug Deliv Rev. 2003; 55:217–250. [PubMed: 12564978]
15. Lutz JF, Akdemir O, Hoth A. Point by point comparison of two thermosensitive polymers exhibiting a similar LCST: Is the age of poly(NIPAM) over? J Am Chem Soc. 2006; 128:13046–13047. [PubMed: 17017772]
16. Lutz JF. Polymerization of oligo(ethylene glycol) (meth)acrylates: Toward new generations of smart biocompatible materials. J Polym Sci Part A: Polym Chem. 2008; 46:3459–3470.
17. Cai T, Marquez M, Hu ZB. Monodisperse thermoresponsive microgels of poly(ethylene glycol) analogue-based biopolymers. Langmuir. 2007; 23:8663–8666. [PubMed: 17658862]

18. Banet P, Griesmar P, Serfaty S, Vidal F, Jaouen V, Le Huerou JYL J-Y. One-Shot Synthesis of a Poly(N-isopropylacrylamide)/Silica Hybrid Gel. J Phys Chem B. 2009; 113:14914–14919. [PubMed: 19888763]
19. Schmitz, KS. An introduction to dynamic light scattering by macromolecules. Boston: Academic Press, Harcourt Brace Jovanovich Publishers; 1990.
20. Berne, BJ.; Pecora, R. Dynamic light scattering: with applications to chemistry, biology, and physics. New York: Wiley Interscience; 1976.
21. Provencher SW. Inverse Problems in Polymer Characterization - Direct Analysis of Polydispersity with Photon Correlation Spectroscopy. Macromol Chem Phys. 1979; 180:201–209.
22. Gao J, Hu ZB. Optical properties of N-isopropylacrylamide microgel spheres in water. Langmuir. 2002; 18:1360–1367.
23. Chen JL, Chiang CH, Yeh MK. The mechanism of PLA microparticle formation by water-in-oil-in-water solvent evaporation method. J Microencapsul. 2002; 19:333–346. [PubMed: 12022499]
24. Kamath S, Bhattacharyya D, Padukudru C, Timmons RB, Tang L. Surface chemistry influences implant-mediated host tissue responses. J Biomed Mater Res A. 2008; 86A:617–626. [PubMed: 18022841]
25. Nair A, Zou L, Bhattacharyya D, Timmons RB, Tang L. Species and density of implant surface chemistry affect the extent of foreign body reactions. Langmuir. 2008; 24:2015–2024. [PubMed: 18189430]
26. Sheffield JB. ImageJ, a useful tool for biological image processing and analysis. Microsc Microanal. 2007; 13:200–201.
27. Yoshimura A, Ohnishi S. Uncoating of Influenza-Virus in Endosomes. J Virol. 1984; 51:497–504. [PubMed: 6431119]
28. Xia XH, Hu ZB, Marquez M. Physically bonded nanoparticle networks: a novel drug delivery system. J Control Release. 2005; 103:21–30. [PubMed: 15710497]
29. Weng H, Zhou J, Tang L, Hu ZB. Tissue responses to thermally-responsive hydrogel nanoparticles. J Biomat Sci-Polym E. 2004; 15:1167–1180.
30. Gulati N, Rastogi R, Dinda AM, Saxena R, Koul V. Characterization and cell material interactions of PEGylated PNIPAAM nanoparticles. Colloid Surface B. 2010; 79:164–173.
31. Yang A, Liu W, Li Z, Jiang L, Xu H, Yang X. Influence of polyethyleneglycol modification on phagocytic uptake of polymeric nanoparticles mediated by immunoglobulin G and complement activation. J Nanosci Nanotechnol. 2010; 10:622–628. [PubMed: 20352902]
32. Herten M, Jung RE, Ferrari D, Rothamel D, Golubovic V, Molenberg A, et al. Biodegradation of different synthetic hydrogels made of polyethylene glycol hydrogel/RGD-peptide modifications: an immunohistochemical study in rats. Clin Oral Implan Res. 2009; 20:116–125.
33. Reis CP, Ribeiro AJ, Houng S, Veiga F, Neufeld RJ. Nanoparticulate delivery system for insulin: Design, characterization and in vitro/in vivo bioactivity. Eur J Pharm Sci. 2007; 30:392–397. [PubMed: 17280820]
34. Polli JE. In vitro studies are sometimes better than conventional human pharmacokinetic in vivo studies in assessing bioequivalence of immediate-release solid oral dosage forms. AAPS J. 2008; 10:289–299. [PubMed: 18500564]
35. Weissleder R, Tung CH, Mahmood U, Bogdanov A Jr. In vivo imaging of tumors with protease-activated near-infrared fluorescent probes. Nat Biotechnol. 1999; 17:375–378. [PubMed: 10207887]
36. Rao J, Dragulescu-Andrasi A, Yao H. Fluorescence imaging in vivo: recent advances. Curr Opin Biotechnol. 2007; 18:17–25. [PubMed: 17234399]
37. Liu S, Jia B, Qiao R, Yang Z, Yu Z, Liu Z, et al. A novel type of dual-modality molecular probe for MR and nuclear imaging of tumor: preparation, characterization and in vivo application. Mol Pharm. 2009; 6:1074–1082. [PubMed: 19527074]
38. Lee JY, Kang YM, Kim ES, Kang ML, Lee B, Kim JH, et al. In vitro and in vivo release of albumin from an electrostatically crosslinked in situ-forming gel. J Mater Chem. 2010; 20:3265–3271.
39. Smitha B, Sridhar S, Khan AA. Polyelectrolyte complexes of chitosan and poly(acrylic acid) as proton exchange membranes for fuel cells. Macromolecules. 2004; 37:2233–2239.

40. Hu Y, Jiang XQ, Ding Y, Ge HX, Yuan YY, Yang CZ. Synthesis and characterization of chitosan-poly(acrylic acid) nanoparticles. Biomaterials. 2002; 23:3193–3201. [PubMed: 12102191]
41. Ikawa T, Abe K, Honda K, Tsuchida E. Interpolymer Complex between Poly(Ethylene Oxide) and Poly(Carboxylic Acid). J Polym Sci Part A: Polym Chem. 1975; 13:1505–1514.
42. Oyama HT, Tang WT, Frank CW. Complex-Formation between Poly(Acrylic Acid) and Pyrene-Labeled Poly(Ethylene Glycol) in Aqueous-Solution. Macromolecules. 1987; 20:474–480.
43. Kim SY, Kim HJ, Lee KE, Han SS, Sohn YS, Jeong B. Reverse thermal gelling PEG-PTMC diblock copolymer aqueous solution. Macromolecules. 2007; 40:5519–5525.
44. Fechler N, Badi N, Schade K, Pfeifer S, Lutz JF. Thermogelation of PEG-Based Macromolecules of Controlled Architecture. Macromolecules. 2009; 42:33–36.
45. Badi N, Lutz JF. PEG-based thermogels: applicability in physiological media. J Control Release. 2009; 140:224–229. [PubMed: 19376170]
46. Hoffmann J, Groll J, Heuts J, Rong H, Klee D, Ziemer G, et al. Blood cell and plasma protein repellent properties of Star-PEG-modified surfaces. J Biomat Sci-Polym E. 2006; 17:985–996.
47. Yang X, Kim JC. beta-Cyclodextrin Hydrogels Containing Naphthaleneacetic Acid for pH-Sensitive Release. Biotechnol Bioeng. 2010; 106:295–302. [PubMed: 20148415]
48. Nam K, Watanabe J, Ishihara K. The characteristics of spontaneously forming physically cross-linked hydrogels composed of two water-soluble phospholipid polymers for oral drug delivery carrier I: hydrogel dissolution and insulin release under neutral pH condition. Eur J Pharm Sci. 2004; 23:261–270. [PubMed: 15489127]
49. Rasool N, Yasin T, Heng JYY, Akhter Z. Synthesis and characterization of novel pH-, ionic strength and temperature-sensitive hydrogel for insulin delivery. Polymer. 2010; 51:1687–1693.
50. Yin L, Ding J, Zhang J, He C, Tang C, Yin C. Polymer integrity related absorption mechanism of superporous hydrogel containing interpenetrating polymer networks for oral delivery of insulin. Biomaterials. 2010; 31:3347–3356. [PubMed: 20116843]

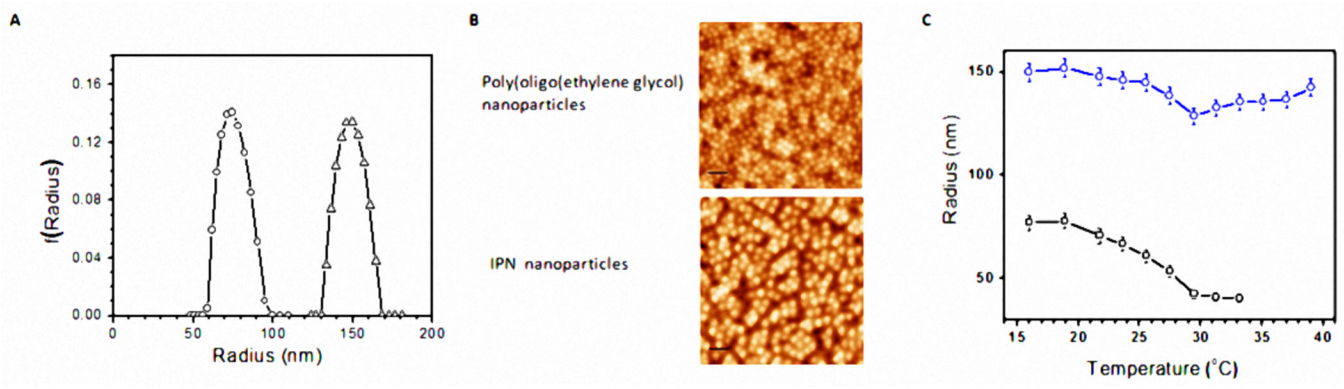

Figure 1.

(a) Size distributions of poly(oligo(ethylene glycol)) (circles) and its IPN nanoparticles (triangles) at 21°C. (b) AFM images of dehydrated poly(oligo(ethylene glycol)) nanoparticles and its IPN nanoparticles. The scale bar is 250 nm. (c) Temperature-dependent radii of poly(oligo(ethylene glycol)) and its IPN nanoparticles (circles) and (triangles) in water.

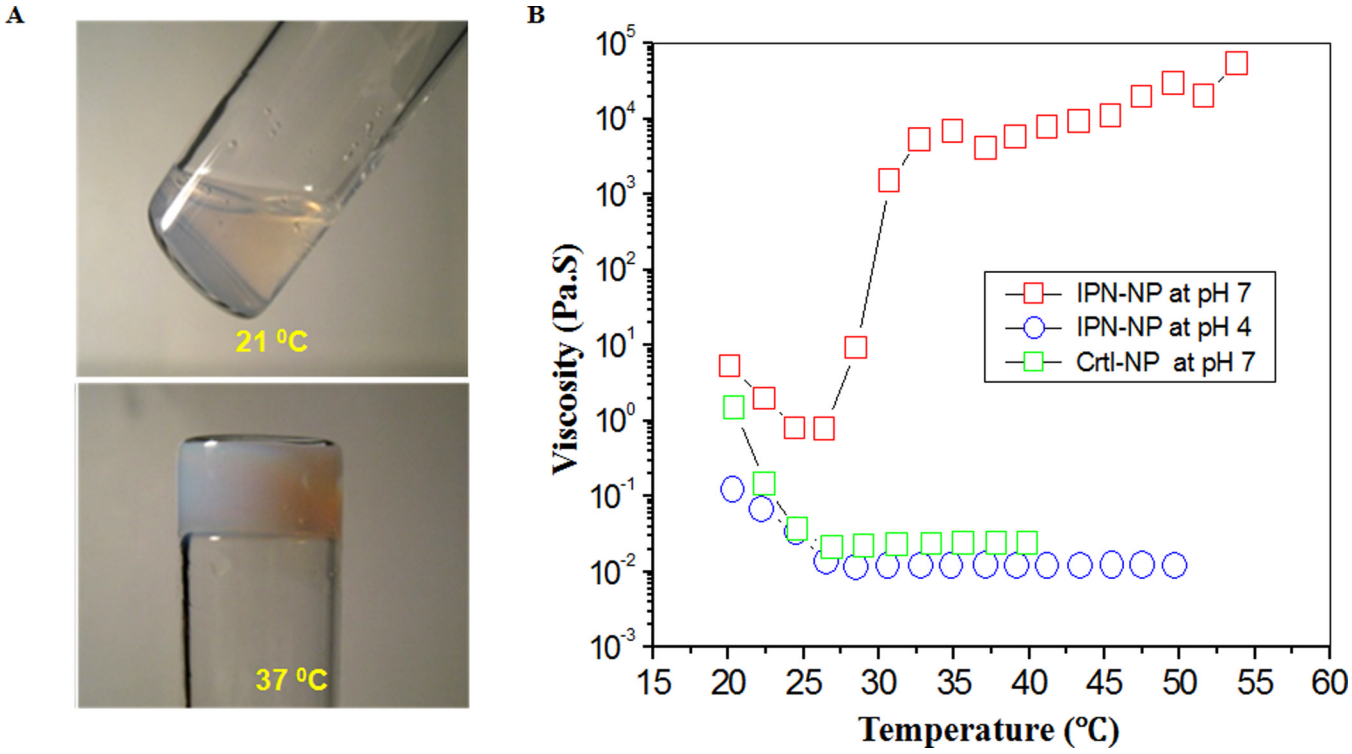

Figure 2.

(A) Thermogelling effect: The dispersion of IPN nanoparticles is a fluid at 21°C but is physically gelled and could not flow at 37 °C. (B) Temperature/pH dependent viscosity of dispersions of polymer nanoparticles (5%wt) of poly(oligo(ethylene glycol)) and its IPN nanoparticles. The thermogelling effect occurs only for IPN nanoparticles at pH 7.

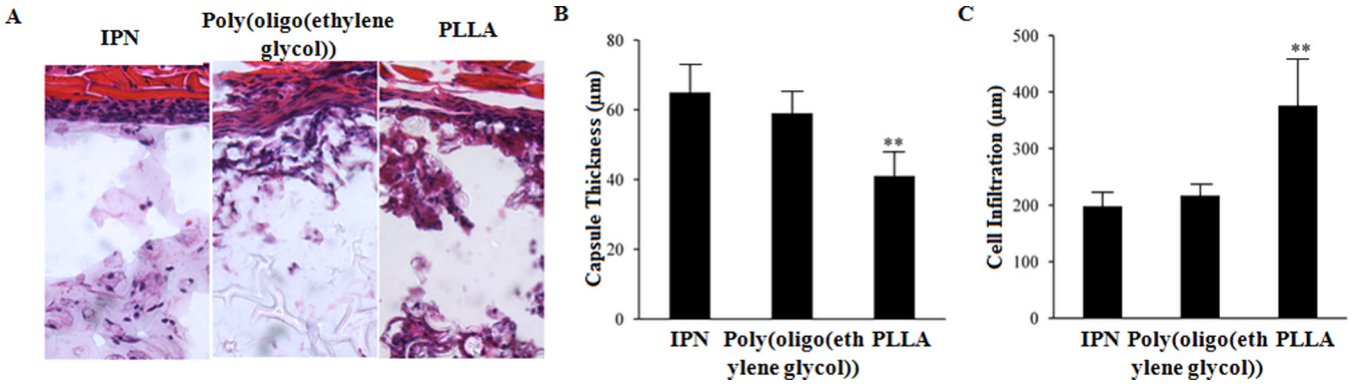

Figure 3.

Assessment of tissue responses to IPN nanoparticles in mice. Test materials (poly(oligo(ethylene glycol)) and its IPN nanoparticles, PLLA microparticles as control) were subcutaneously implanted on Balb/C mice. After implantation for 2 weeks, the implants and surrounding tissues were recovered for histological analyses. H&E stain shows that (A) IPN nanoparticles and poly(oligo(ethylene glycol)) nanoparticles prompt similar and minimal extent of tissue responses with little cell infiltration. On the other hand, PLLA particles triggered stronger cell responses which led to more cell infiltration into the particle implants. (B) PLLA particle implants were found to prompt >50% more cell infiltration than poly(oligo(ethylene glycol))-based nanoparticles supporting the cell repelling properties of PEG. (C) On the other hand, most of the recruited cells stayed in the capsule region of the IPN nanoparticle and poly(oligo(ethylene glycol)) nanoparticle implants caused the increase in capsule thickness by comparison with PLLA particle implants. N=5. Significance of various particles *vs.* IPN particles, ** $P \leq 0.01$.

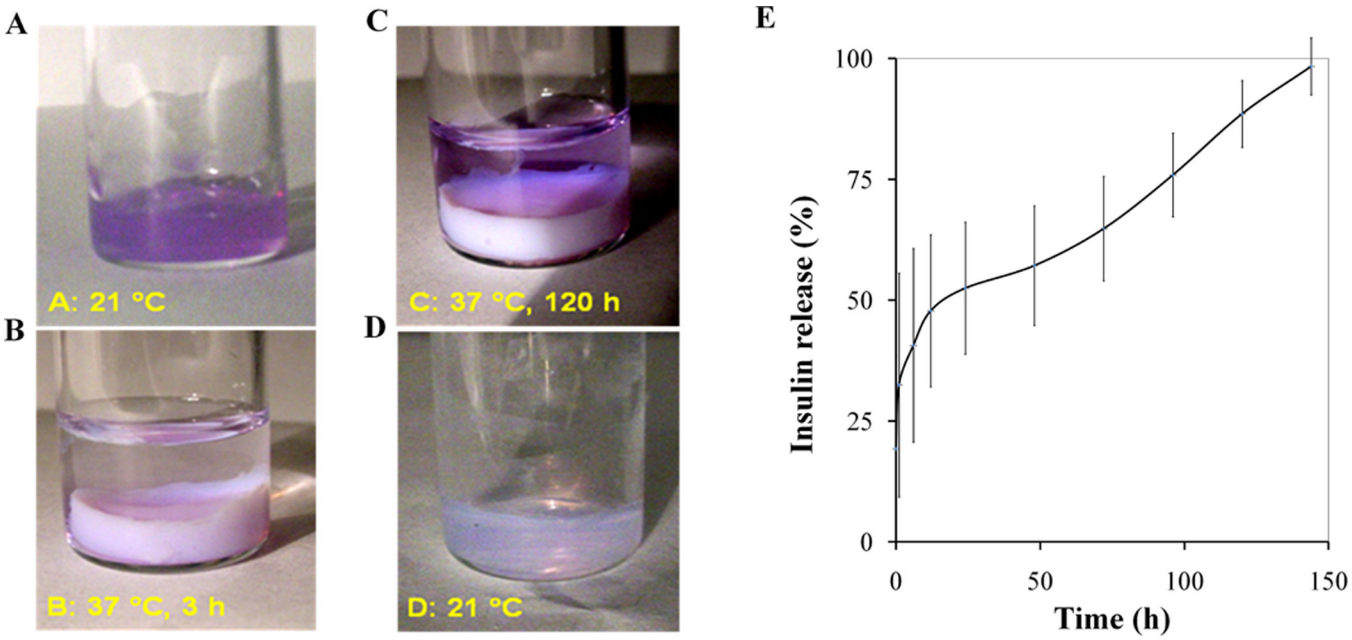

Figure 4.

Controlled release of Texas red dye-conjugated dextran and insulin from IPN hydrogel *in vitro*. Slow release of Texas red dye-conjugated dextran was monitored via visual observation. Specifically, (A) at 21 °C, the Texas red dye-conjugated dextran was mixed with the dispersion of IPN nanoparticles. (B) When temperature was increased to 37 °C, the Texas red dyeconjugated dextran was trapped inside the solid-like gel. By addition of phosphate-buffered saline (PBS: pH 7.4) on top of the dye-trapped gel for three hours, a small amount of Texas red dye-conjugated dextran was released into the PBS solution. (C) After 120 h, more dye can be seen in solution and less dye was found residing inside the gel. (D) After removal of the supernatant/PBS solution, the gel was cooled to 21 °C at which the solid-like gel transitioned into liquid state. A separate study was carried out to quantify the slow release of insulin from the IPN nanoparticles. (E) The average percentage of insulin released from the gel of IPN nanoparticles at 37 °C. The error bars represent the standard deviation of the compiled measurements of all three samples.

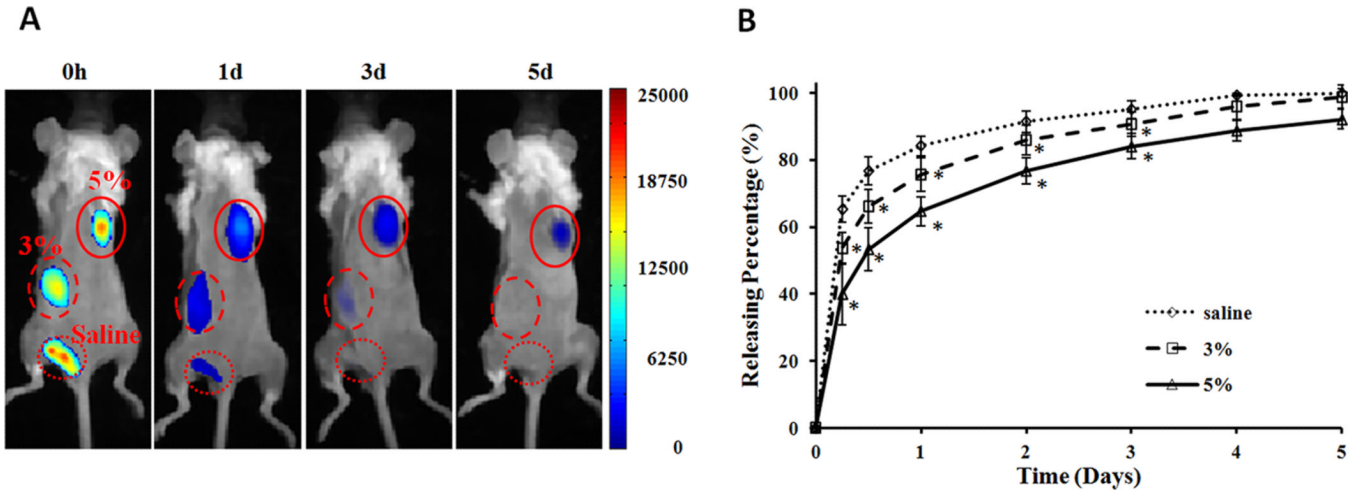

Figure 5.

In vivo quantification of protein release from IPN hydrogel. NIR dye-labeled BSA were mixed with different concentrations (0, 3, and 5% polymer weight) of IPN nanoparticles (1 mg BSA/100 μl nanoparticles) at room temperature and then implanted subcutaneously on the back of a mouse. (A) *In vivo* images represent the fluorescence intensities of different implantation sites at specified time points (0, 1, 3, and 5 days). (B) Quantification of the percentages of accumulative release of NIR-BSA from different concentration of IPN nanoparticles up to day 5.